Hydrogen in the Deep Earth

Jed Mosenfelder, Hélène Bureau, Anthony C Withers

Hydrogen in the Deep Earth

Jed L. Mosenfelder[1], Hélène Bureau[2], and Anthony C. Withers[3]

ABSTRACT

Hydrogen remains one of the most difficult elements to characterize in geological materials. Even at trace levels, it has a major impact on the properties of minerals, silicate melts, and fluids, and thus on the physical state of the mantle and the crust. The investigation of H-bearing species in deep minerals, melts and fluids is challenging because these phases can be strongly modified during transport to Earth´s surface. Furthermore, interpretation of experimental studies can be clouded by kinetic inhibitions and other artifacts. Nevertheless, recent improvements in analytical, experimental, and modeling methodologies have enabled advances in our understanding of how hydrogen is incorporated in the deep Earth, which is essential for constraining hydrogen cycling and storage through geologic time.

KEYWORDS: water; mantle; incorporation; speciation

[1] Planetary Science Institute

1700 E. Fort Lowell

Tucson, AZ 85719, USA

E-mail: jmosenfelder@psi.edu

[2] Institut de Minéralogie, de Physique des Matériaux
et de Cosmochimie (IMPMC)
Sorbonne Université
CNRS UMR 7590
Muséum National d'Histoire Naturelle
4 Place Jussieu
75252 Paris Cedex 05, France
E-mail: helene.bureau@upmc.fr

[3] Bayerisches Geoinstitut

Universität Bayreuth

D-95440 Bayreuth, Germany

E-mail: tony.withers@uni-bayreuth.de

INTRODUCTION

Hydrogen is one of the most difficult elements to characterize in geological materials, partly because it is often only a trace component in minerals that are defined as nominally anhydrous, with no hydrogen in their chemical formula (hereafter referred to as NAMs). Yet hydrogen, even at trace levels, has a major impact on the properties of minerals, silicate melts and fluids, and consequently on the evolution and physical state of the interior of the Earth and other planetary bodies. The distribution of hydrogen in Earth's deep interior and its evolution over geologic time will be covered in later chapters of this Elements issue. We focus here on current challenges to measuring ppm levels (see sidebar for a discussion of units used in this issue) of hydrogen and recent advancements in understanding how it is incorporated in the deep Earth, concentrating on NAMs, fluids, and melts in the mantle while neglecting the important role of hydrous minerals in the crust and upper mantle.

The incorporation mechanisms of hydrogen in mantle minerals, fluids and melts depend on many factors, including pressure, temperature, chemistry and redox conditions. This dependence generates a variety of H-bearing species, from oxidized to reduced, which in theory can be used to map deep mantle redox conditions if they are not altered during transport to the Earth's surface. The analysis of hydrogen in minerals, quenched melts, and inclusions in diamond that preserve evidence of deep-seated hydration has seen major improvements in the past two decades. Concurrently, efforts are continuously being devoted to developing and combining analytical, experimental and modeling methodologies to describe the incorporation and transport processes for hydrogen in mineral structures, silicate melt networks and fluids. These are necessary requisites to improve our understanding of deep hydrogen cycling and storage through geologic time.

MEASURING HYDROGEN

Despite being the most abundant element in the universe – and in part, because of its abundance – hydrogen presents challenges for quantitative measurement. At ppm levels in particular, attention should be paid to contamination by H-bearing species in an instrument vacuum, surface-adsorbed water, and organic molecules on surfaces introduced during sample preparation. Rossman (2006) provided a comprehensive review of the advantages and limitations of the many techniques used

for trace H analysis in NAMs and glasses, including absorption Fourier transform infrared spectroscopy (FTIR), thermogravimetric analysis (TGA), P_2O_5 coulometry, Karl-Fischer titration, hydrogen manometry, continuous-flow mass spectrometry, nuclear reaction analysis (NRA), elastic recoil detection analysis (ERDA), proton-proton (p-p) scattering, nuclear magnetic resonance (NMR), and secondary ion mass spectrometry (SIMS). Since the time of that review, there have been major advances in instrumentation and analytical protocols for some of these techniques.

FTIR is still the most popular of these methods, with advantages including low cost, wide availability, and low detection limits for suitably prepared samples. Moreover, FTIR provides constraints on incorporation mechanisms (structural sites and speciation) for H in minerals and glasses that none of the other techniques above besides NMR yield directly. This information can be deduced from the frequency dependence and – for anisotropic minerals – polarization of IR absorption bands (FIG. 1). SIMS has emerged as the second most frequently used technique, with improvements in detection limits afforded by advancements in instrumentation and protocol (e.g., Mosenfelder et al. 2011). This method also offers the advantage of simultaneous measurement of other elements and isotopes, including other light elements such as fluorine that can also be incorporated at trace levels in NAMs. Furthermore, microbeam techniques such as SIMS and ERDA permit detection of H in phases such as metals or opaque minerals that cannot be readily measured using FTIR. A closely related variant of SIMS is NanoSIMS, which offers superior imaging capability and increased spatial resolution (by a factor of at least two, depending on the detection limit needed – for instance, NAMs from xenoliths can be suitably analyzed with an 8-10 μm diameter area with SIMS, or a 3-5 μm area using NanoSIMS). NanoSIMS in imaging mode can also be useful for assessing the presence of sub-micrometer to micrometer scale features – such as fluid inclusions or inclusions of hydrous phases or hydrous melt – that can skew interpretation in both natural (Mosenfelder et al. 2011) and synthetic (e.g., Liu et al. 2021) samples.

A critical limitation of both FTIR and SIMS that is sometimes misunderstood is that neither of these techniques can yield accurate concentrations without reference to an external calibration by an independent technique, preferably on a material with a composition (and structure, particularly for FTIR) similar to the unknown. Molar absorption coefficients for bands in FTIR spectra vary for materials with different compositions. Ion yields used in SIMS for quantification fundamentally depend on the major element composition of the material being analyzed, and the magnitude of this

"matrix effect" is still poorly constrained for measurements of hydrogen concentration. "Absolute" techniques that have been used to empirically calibrate FTIR and SIMS include hydrogen manometry and nuclear techniques (NRA, ERDA, p-p scattering).

Improvements in spatial resolution, data handling, and detection limits have been made in ERDA in the past 15 years (FIG. 2), and this method has been used to establish FTIR calibrations for H in some of the most important minerals in the deep Earth, including olivine (Withers et al. 2012) and its high-pressure polymorphs wadsleyite and ringwoodite (Bolfan-Casanova et al. 2018). The Withers et al. (2012) calibration results in lower hydrogen concentrations (by a factor of 0.63) in olivine compared to a previous calibration based on NRA measurements of natural olivines, which may have suffered from complications caused by sub-micrometer sized inclusions of hydrous phases (Mosenfelder et al. 2011). For the high-pressure polymorphs, in contrast, the new ERDA-based calibrations result in higher hydrogen concentrations compared to calibrations that were used in the past. These older calibrations were derived to quantify the well-known fact that absorption intensities vary with frequency of the O-H stretching vibration, but subsequent studies demonstrated that they can over- or underestimate hydrogen concentrations in non-systematic ways for different minerals (Rossman 2006). More work is needed to constrain the magnitude of the frequency dependence of IR molar absorption coefficients, which could be important for minerals like olivine with variable IR spectra encompassing a wide frequency range (FIG. 1).

Technical improvements are also in progress for p-p scattering, which has the advantage of revealing the 3-dimensional distribution of hydrogen in thin samples. This capability could be used to detect hydrous inclusions in samples and is effective for discriminating against surface contamination (Weis et al. 2018). Another, more commonly used technique in geoscience is Raman spectroscopy. Raman is a particularly powerful technique for characterizing hydrogen speciation in fluid inclusions (e.g., Vlasov et al. 2023) and H_2O concentrations in melt inclusions (Thomas et al. 2006) that are not exposed at the surface of a mineral. The introduction of higher power lasers has also made it more feasible to quantify hydrogen in NAMs (e.g., Thomas et al. 2015; Martinek and Bolfan-Casanova 2021), although this method can be difficult to apply accurately owing to variations in laser power and other instrumental factors that need to be carefully controlled. Nevertheless, Raman can be especially useful for small phases with high H contents that are difficult to measure otherwise, simultaneously providing site-specific information analogous to that

provided by FTIR.

HYDROGEN IN MANTLE MINERALS

Upper mantle

Hydrogen in deep-seated minerals is most commonly incorporated as hydroxyl (OH^-), although other mechanisms involving structurally bound H_2O, various configurations of H bonded to C (in diamonds; Vangu et al. 2023) or N (as NH_4^+), and even neutral H_2 molecules (Yang et al. 2016) can also be relevant. Structural sites for OH^- are well defined for hydrous phases such as amphibole, but in NAMs the sites can vary considerably even for a single mineral. This variation can provide clues to the physical conditions at which the mineral last equilibrated. Hydrogen in NAMs can be incorporated via coupled substitution with other elements, or in association with intrinsic point defects such as vacancies in cation sites.

Taking olivine as an example, FIGURE 1 illustrates most of the IR absorption bands commonly observed in natural and synthetic crystals that have not been otherwise attributed to fluid inclusions or inclusions of hydrous phases such as serpentine. The comparison demonstrates that absorption bands in natural crystals can be reproduced in experiments. Moreover, the stark difference between spectra of two different natural olivines derived from the mantle implies that no single incorporation mechanism can be called upon to explain all the bands. Indeed, the structural sites responsible for the different absorptions in these samples are still vigorously debated, with proposed mechanisms including vacancies in octahedral or tetrahedral sites balanced by protonation of oxygen atoms, coupled substitutions with Al^{3+} or Fe^{3+} in octahedral sites paired with vacancies in adjacent octahedral sites, coupled substitution with Ti^{4+} or Fe^{3+} in octahedral sites balanced by hydrogen in tetrahedral vacancies, and various coupled substitutions of hydrogen with fluorine or boron.

More effort has been invested into olivine than any other NAM for the purpose of studying the effects of pressure, temperature, oxygen fugacity, and other thermodynamic parameters (e.g., silica activity, H_2O and CO_2 fugacity) on hydrogen incorporation. In theory, spectral characteristics and overall H content could be used to infer conditions of formation for mantle samples, but

discrepancies among studies prevent consensus on an overall thermodynamic law. Some of these discrepancies can be attributed to the use of different analytical methods and calibrations, but some are probably related to incomplete approach to equilibrium caused by slow diffusion kinetics. Hydrogen diffusion mechanisms in olivine and other NAMs have been intensely investigated and are more complex than originally thought, with complications caused by different diffusion rates for and intersite-reaction between different defects (Padrón-Navarta et al. 2014; Jollands et al. 2019). Thus, the distribution of point defects in the starting material can lead to a metastable OH^- pattern in FTIR spectra, if there is insufficient time in the experiment to reach true equilibrium.

A further complication is that "solubility" experiments in simple systems (e.g., one or two mineral phases plus fluid) cannot be used to accurately model the storage capacities of NAMs in natural peridotites or other rocks, because the presence of multiple phases changes water fugacities as a result of varying dissolution of chemical species into the coexisting fluid, melt, or supercritical fluid. Consequently, studies constraining H contents and partitioning between multiple NAMs (olivine, orthopyroxene, clinopyroxene, and garnet) and coexisting hydrous melts at high pressure are critical for determining the overall H storage capacity of the mantle and the influence of hydrogen on the onset of partial melting (e.g., Novella et al. 2014). These studies reveal that H storage capacity in olivine goes up with increasing depth, while storage capacity in pyroxenes declines with increasing depth as a result of decreasing Al solubility with increasing pressure. Furthermore, the H storage capacity of garnets with pyrope-rich compositions relevant to the mantle is much lower than other NAMs, despite the fact that grossular-rich crustal garnets can contain wt% levels of H_2O.

Recent improvements in analytical techniques (FIG. 2) have facilitated quantification of H contents in diamonds, revealing H to be the second major impurity in between N and B (Vangu et al. 2023). Although diamonds are minor phases in the mantle, they can be used to place constraints on parent metasomatic fluids. Combined investigations of hydrogen in host diamonds and their fluid and solid inclusions (e.g., Pearson et al. 2014; Tschauner et al. 2018; Weiss et al. 2022) from cratons, the transition zone and the lower mantle thus could constitute a powerful strategy to characterize hydrogen cycling in the deep Earth (Novella et al. 2024 this issue).

Transition zone

The dominant phases in the mantle transition zone between 410 and 660 km depth are the high-pressure polymorphs of olivine (wadsleyite and ringwoodite) and majoritic garnet, with minor amounts of clinoenstatite or akimotoite depending on pressure, temperature, and whole-rock composition. It has been recognized for over 30 years from theoretical and experimental studies that wadsleyite and ringwoodite could be significant hosts for hydrogen. Experiments demonstrate that they can incorporate weight percent levels of H_2O (up to ~3 wt% H_2O; e.g., Bolfan-Casanova et al. 2018), far beyond the amounts that can be stored in olivine and other NAMs at lower pressures. Significantly lower, but non-trivial amounts of hydrogen can be incorporated in majorite (up to ~1000 ppm H_2O; e.g., Thomas et al. 2015), clinoenstatite, and akimotoite. The importance of these phases as carriers for hydrogen in the deep Earth has now been field tested by the discovery of a hydrous ringwoodite inclusion (containing ~1.5 wt% H_2O) in diamond (Pearson et al. 2014), proving that at least locally the transition zone is a rich hydrous reservoir in the deep Earth.

Recognition of the capacity of the transition zone to store more hydrogen than the upper mantle has spurred numerous attempts to constrain its actual hydrogen content using seismology and electrical conductivity. Furthermore, the low velocity zone above the 410 km seismic discontinuity can be conveniently explained as a consequence of dehydration melting caused by the upwelling of hydrated transition zone material. This low velocity zone in turn forms a source for hydrated melts that can ascend further once they become buoyant, balancing the influx of water into the transition zone from subducting slabs. Geophysical and geochemical implications of a "wet" transition zone are explored later in this issue.

Lower mantle

Deeper still in the Earth, potentially the most important carrier for hydrogen is bridgmanite, the perovskite-structured polymorph of orthopyroxene that comprises ~80% of the mantle below the transition zone. Unfortunately, experimental studies on hydrogen incorporation in bridgmanite are highly contradictory. Some studies have suggested this mineral can incorporate as much as 0.1-0.2 wt% H_2O, if H associated with Al^{3+} or Fe^{3+} replaces Si^{4+} in the structure (e.g., Fu et al. 2019). However, other studies (e.g., Liu et al. 2021) have measured much lower or completely negligible H concentrations and proposed that other measurements by SIMS or FTIR were compromised by the presence of hydrous phases or melt, either as inclusions in bridgmanite or on grain boundaries between crystals. This concern may also apply to claims of relatively high hydrogen concentrations in periclase (or ferropericlase) and davemaoite ($CaSiO_3$ perovskite), the next most prevalent

minerals in the lower mantle.

If bridgmanite and other NAMs comprising the bulk of the lower mantle can't incorporate significant hydrogen, the best candidates for transporting hydrogen into the deepest parts of the Earth may be dense hydrous magnesium-aluminum silicates (such as phase D and phase H, with variable Al contents), aluminous or ferric phases (such as δ-AlOOH and the high-pressure polymorphs of FeOOH), or solid solutions between these phases (e.g., Nishi et al. 2017; Ishii et al. 2022). These high-pressure phases are unstable along average mantle adiabats but can be stable within cold subducting slabs.

Another phase relevant in subducting slabs is stishovite, stable at pressures above ~9 GPa. Earlier experiments revealed low storage capacities for hydrogen in this SiO_2 polymorph, primarily tied to the presence of Al^{3+} impurities. However, an "ultrahydrous" form of stishovite containing weight-percent levels of H_2O can be synthesized at low temperatures (350-550 °C, at ~10 GPa; Spektor et al. 2016). This ultrahydrous stishovite is also stable at higher temperatures and pressures and comparable amounts of hydrogen may also be incorporated in the higher-pressure $CaCl_2$-structured SiO_2 polymorph (e.g., Lin et al. 2022). However, the exact amounts are subject to large uncertainties as they are primarily based on density functional theory (DFT) calculations and/or calculations from X-ray diffraction (XRD) data combined with extrapolated equations of state for the ultrahydrous phase. Furthermore, coupled substitution of Al^{3+} and H^{+} becomes increasingly feasible at more extreme conditions (Ishii et al. 2022). Thus, stishovite and its higher-pressure polymorphs, with a wide combined pressure-temperature stability, could facilitate transport of hydrogen from the upper mantle all the way down to the core-mantle boundary. Dehydration, melting, and/or reaction with liquid iron to form iron hydride phases would then likely occur at the thermal boundary layer next to the outer core (Lin et al 2022).

HYDROGEN IN FLUIDS AND MELTS

Aqueous fluids and hydrous melts are key transport agents for hydrogen in the Earth. At certain pressures and temperatures in the upper mantle, fluids and melts become miscible (supercritical), with important geophysical and geochemical implications (e.g., Mibe et al. 2007). Advances in analytical techniques and high-pressure instrumentation are opening up new avenues for studying

deep-seated fluids and hydrous melts. For instance, synchrotron XRD enabled the discovery of Ice-VII inclusions in diamonds that were trapped at pressures as high as 25 GPa (Tschauner et al. 2018). This finding supports the inference from hydrous ringwoodite in diamond (Pearson et al. 2014) that localized regions of the transition zone (and possibly the top of the lower mantle) are hydrated. More broadly, the application of a battery of microanalytical techniques including FTIR, Raman, electron microprobe analysis, and electron microscopy assisted by focused ion-beam sample preparation has enabled thorough characterization of complex fluid inclusions in natural lithospheric diamonds, as reviewed by Weiss et al. (2022).

On the experimental side, progress in understanding the speciation of fluids in the deep Earth is exemplified by studies of synthetic fluid inclusions (Vlasov et al. 2023). This work demonstrates immiscibility between H_2 and H_2O at high pressures, which potentially has important implications for the overall oxidation of the mantle early in Earth's evolution and diamond growth in super-reducing environments in the modern Earth (Vlasov et al. 2023). Although technically still very difficult, high-pressure experiments using synchrotron XRD (in a large volume press; Mibe et al. 2007) and other in situ techniques (e.g., spectroscopic observations in diamond anvil cells) have also made remarkable progress in directly observing supercritical behavior in deep fluids and melts.

Decades of research have gone into understanding the dissolution mechanisms of hydrogen in glasses quenched from melts at high pressure, but recent advances reveal new complexities with important implications for the geochemical evolution of the Earth. The prevailing wisdom that hydrogen dissolves in geologically relevant melts primarily as either molecular H_2O or OH^- groups has been overturned by experiments (Hirschmann et al. 2012) demonstrating that molecular H_2 can be a dominant species at high pressure and low oxygen fugacity (FIG. 3). Furthermore, a wealth of new experimental studies (e.g., Grewal et al. 2020) have revealed that low oxygen fugacities promote complexing of hydrogen with carbon and nitrogen. The solubility of H_2 and various C-H and N-H species (example shown in FIG. 3) in melts as a function of thermodynamic variables is a complex topic beyond the scope of this paper, but the recognition of these incorporation mechanisms has critical implications for the distribution of volatiles in planetary bodies and their degassing and redox evolution following magma ocean formation and solidification (e.g., Hirschmann et al. 2012; Grewal et al. 2020).

The development of a new rapid-quenching multi-anvil technique (FIG. 3) has facilitated study of previously unquenchable depolymerized melts, including peridotitic glasses that are directly relevant to the lower mantle (Bondar et al. 2023). It has long been known that the relative proportions of H_2O and OH^- groups depend on melt composition and overall hydrogen content, but this new work demonstrates previously unseen complexities in bands attributed to the OH^- groups (FIG. 3). In peridotitic glasses, two bands at 4400 and 4270 cm^{-1} are observed, as opposed to the single band between ~4500 to 4400 cm^{-1} in more polymerized glasses. These bands are interpreted to represent (Si,Al)-OH and (Ca,Mg)-OH species, respectively, whereas the single band is interpreted to represent only (Si,Al)-OH. The appearance of new species in increasingly depolymerized glasses and the frequency shifts will require further work to determine the absorption coefficients for the bands and establish a solubility law at very high pressures that is more relevant to melting in the deep Earth. Ultimately, this finding will have critical implications for modeling not only water-fluxed formation of ultramafic melts, but hydrogen solubility in magma oceans, which influences planetary degassing (e.g., Hirschmann et al. 2012).

CONCLUSION

The study of hydrogen in the deep Earth will continue to advance via improvements in experimental instrumentation, analytical techniques, and quantitative modeling, only some of which we have been able to cover here. For instance, we have almost completely ignored DFT-based, first-principles predictions of hydrogen incorporation mechanisms and storage capacities at high pressures and temperatures. These studies will inevitably play an increasingly important role as computing power grows. On the analytical side, an example of an emerging and promising technique is atom probe tomography (APT), which can be used to hone in on the atomic scale to identify hydrogen incorporation mechanisms. Confident application of APT to NAMs will require overcoming technical limitations (particularly high H backgrounds) with commercially available instruments (Chen et al. 2023). Developments in high-pressure experimentation can also be expected to enable further strides in constraining how hydrogen is recycled and stored in the deep Earth. These developments include both "offline" instrumentation advances in obtaining higher pressures with larger samples, and "online" combination of high-pressure techniques with in situ analytical probes (e.g., synchrotron radiation), allowing the study of hydrogen incorporation in materials while circumventing any chemical or structural modifications caused by quenching.

ACKNOWLEDGMENTS

We are grateful for constructive reviews by E. Libowitzky and H. Skogby, as well as editing by S. Demouchy and H. Keppler.

REFERENCES

Bolfan-Casanova N and 6 coauthors (2018) Examination of water quantification and incorporation in transition zone minerals: wadsleyite, ringwoodite and phase D using ERDA (elastic recoil detection analysis). Frontiers in Earth Science 6: 75. doi: 10.3389/feart.2018.00075

Bondar D, Withers AC, Whittington AG, Fei H, Katsura T (2023) Dissolution mechanisms of water in depolymerized silicate (peridotitic) glasses based on infrared spectroscopy. Geochimica et Cosmochimica Acta 342: 45-61. doi: 10.1016/j.gca.2022.11.029

Chen Y-S and 6 coauthors (2023) Atom probe tomography for the observation of hydrogen in materials: a review. Microscopy and Microanalysis 29: 1-15. doi: 10.1093/micmic/ozac005

Fu S and 10 coauthors (2019) Water concentration in single-crystal (Al,Fe)-bearing bridgmanite grown from the hydrous melt: implications for the dehydration melting at the topmost lower mantle. Geophysical Research Letters 46: 10346-10357. doi: 10.1029/2019GL084630

Grewal DS, Dasgupta R, Farnell A (2020) The speciation of carbon, nitrogen, and water in magma oceans and its effect on volatile partitioning between major reservoirs of the Solar System rocky bodies. Geochimica et Cosmochimica Acta 280: 281-301. doi: 10.1016/j.gca.2020.04.023

Hirschmann MM, Withers AC, Ardia P, Foley NT (2012) Solubility of molecular hydrogen in silicate melts and consequences for volatile evolution of terrestrial planets. Earth and Planetary Science Letters 345-348: 38-48. doi: 10.1016/j.epsl.2012.06.031

Ishii T, Ohtani E, Shatskiy A (2022a) Aluminum and hydrogen partitioning between bridgmanite and high-pressure hydrous phases: implications for water storage in the lower mantle. Earth and Planetary Science Letters 583: 117441. doi: 10.1016/j.epsl.2022.117441

Ishii T and 6 coauthors (2022b) Superhydrous aluminous silica phases as major water hosts in high-temperature lower mantle. Proceedings of the National Academy of Science 119: e2211243119. doi: 10.1073/pnas.2211243119

Jollands MC, Kempf E, Hermann J, Müntener O (2019) Coupled inter-site reaction and diffusion: rapid dehydrogenation of silicon vacancies in natural olivine. Geochimica et Cosmochimica Acta 262: 220-242. doi: 10.1016/j.gca.2019.07.025

Lin Y and 8 coauthors (2022) Hydrous SiO_2 in subducted oceanic crust and H_2O transport to the core-mantle boundary. Earth and Planetary Science Letters 594: 117708. doi: 10.1016/j.epsl.2022.117708

Liu Z and 8 coauthors (2021) Bridgmanite is nearly dry at the top of the lower mantle. Earth and Planetary Science Letters 570: 117088. doi: 10.1016/j.epsl.2021.117088

Mosenfelder JL and 6 coauthors (2011) Analysis of hydrogen in olivine by SIMS: Evaluation of standards and protocol. American Mineralogist 96: 1725-1741, doi: 10.2138/am.2011.3810

Martinek L and Bolfan-Casanova N (2021) Water quantification in olivine and wadsleyite by Raman spectroscopy and study of errors and uncertainties. American Mineralogist 106: 570-580. doi: 10.2138/am-2021-7264

Mibe K and 5 coauthors (2007) Second critical endpoint in the peridotite - H_2O system. Journal of Geophysical Research 112: B0321. doi: 10.1029/2005JB004125

Nishi M, Kuwayama Y, Tsuchiya J, Tsuchiya T (2017) The pyrite-type high-pressure form of FeOOH. Nature 547: 205-208. doi: 10.1038/nature22823

Novella D and 5 coauthors (2014) The distribution of H_2O between silicate melt and nominally anhydrous peridotite and the onset of hydrous melting in the deep upper mantle. Earth and Planetary Science Letters 400: 1-13. doi: 10.1016/j.epsl.2014.05.006

Novella D, Demouchy S, Bolfan-Casanova N (2024) Deep hydrogen reservoirs and longevity. Elements 20(4): XXX-XXX

Padrón-Navarta JA, Hermann J, O'Neill HSC (2014) Site-specific hydrogen diffusion rates in forsterite. Earth and Planetary Science Letters 392: 100-112. doi: 10.1016/j.epsl.2014.01.055

Pearson DG and 11 coauthors (2014) Hydrous mantle transition zone indicated by ringwoodite included in diamond. Nature 507: 221-224. doi: 10.1038/nature13080

Rossman GR (2006) Analytical methods for measuring water in nominally anhydrous minerals. Reviews in Mineralogy and Geochemistry 62: 1–28. doi: 10.2138/rmg.2006.62.1

Spektor K and 7 coauthors (2016) Formation of hydrous stishovite from coesite in high-pressure hydrothermal environments. American Mineralogist 101: 2514-2524. doi: 10.2138/am-2016-5609

Thomas R, Kamanetsky VS, Davidson P (2006) Laser Raman spectroscopic measurements of water in unexposed glass inclusions. American Mineralogist 91: 467-470. doi: 10.2138/am.2006.2107

Thomas S-M and 10 coauthors (2015) Quantification of water in majoritic garnet. American Mineralogist 100: 1084-1092. doi: 10.2138/am-2015-5136

Tschauner O and 10 coauthors (2018) Ice-VII inclusions in diamonds: evidence for aqueous fluid in Earth's deep mantle. Science 359: 1136-1139. doi: 10.1126/science.aao3030

Vangu D and 9 coauthors (2023) Combination of ERDA, FTIR spectroscopy and NanoSIMS for the characterization of hydrogen incorporation in natural diamonds. Diamond & Related Materials 136: 110007. doi: 10.1016/j.diamond.2023.110007

Vlasov K, Audétat A, Keppler H (2023) H_2-H_2O immiscibility in Earth's upper mantle. Contributions to Mineralogy and Petrology 178: 36. doi: 10.1007/s00410-023-02019-7

375 Weis F and 5 coauthors (2018) Hydrogen concentration analysis in clinopyroxene using proton–
376 proton scattering analysis. Physics and Chemistry of Minerals 45: 669-678. doi:
377 10.1007/s00269-018-0953-2

378 Weiss Y, Czas J, Navon O (2022) Fluid inclusions in fibrous diamonds. Reviews in Mineralogy and
379 Geochemistry 88: 475-532. doi: 10.2138/rmg.2022.88.09

380 Withers AC, Bureau H, Raepsaet C, Hirschmann MM (2012) Calibration of infrared spectroscopy by
381 elastic recoil detection analysis of H in synthetic olivine. Chemical Geology 334: 92-98, doi:
382 10.1016/j.chemgeo.2012.10.002

383 Yang X, Keppler H, Li Y (2016). Molecular hydrogen in mantle minerals. Geochemical Perspective
384 Letters 2: 160-168. doi: 10.7185/geochemlet.1616

385

386

Figures

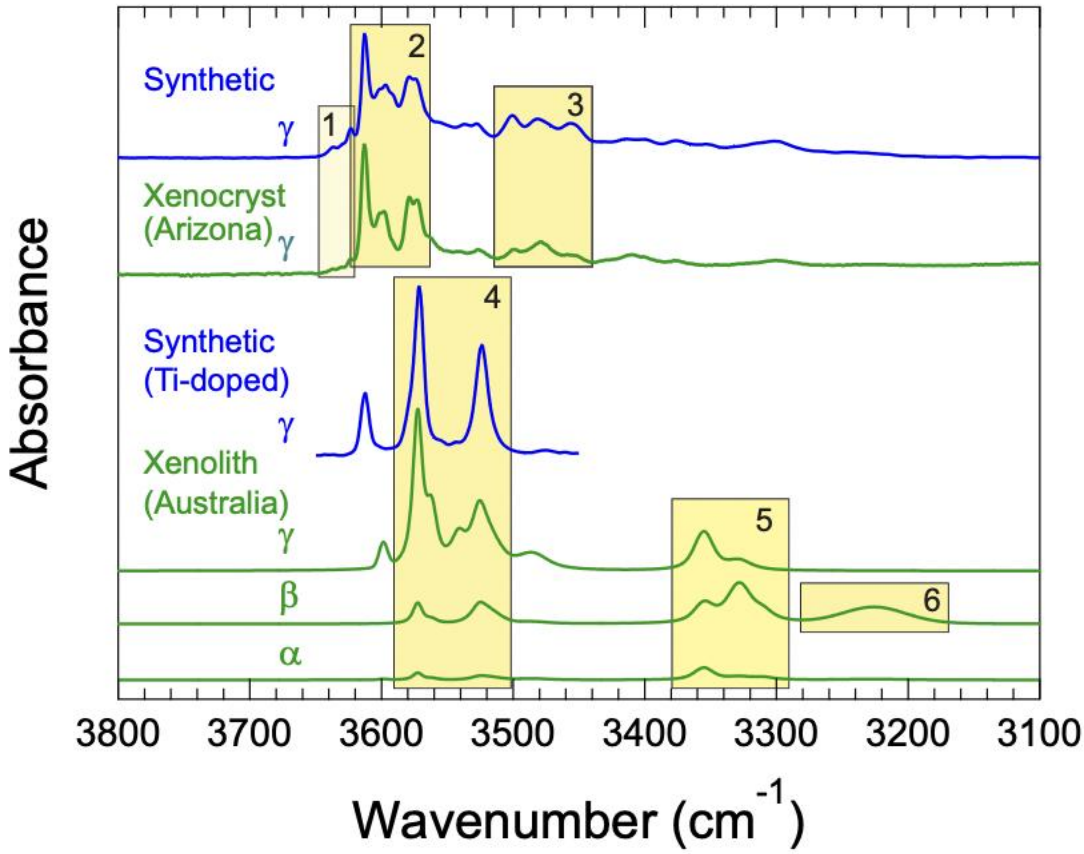

FIGURE 1. Mid-infrared spectra of olivine, illustrating the rich diversity of O-H absorption bands in natural and synthetic crystals. Spectra are arbitrarily scaled and offset for the sake of comparison. Greek letters refer to the optical direction that was parallel to the E-vector of the polarized beam for each spectrum. A strong correspondence is apparent for the spectra of synthetic olivine (recovered from 3 GPa and 1250 °C; Withers et al. 2012) and a xenocryst from Buell Park, Arizona. Spectra for a xenolithic olivine from Mount Gambier, South Australia more closely resemble spectra of synthetic forsterite doped with Ti at 2 GPa and 1400 °C (Padrón-Navarta et al. 2014). Shaded regions denote bands with the following possible interpretations: 1) coupled H-F defects in tetrahedral sites; 2) four H^+ substituting for Si^{4+}; 3) three H^+ substituting for Si^{4+}, with Fe^{2+} in a nearby octahedral site oxidized to Fe^{3+}; 4) two H^+ substituting for Si^{4+}, with Ti^{4+} in a nearby octahedral site; 5) H^+ in a vacant octahedral site, with a trivalent cation (e.g., Al^{3+}, Cr^{3+}, or Fe^{3+}) in an adjacent octahedral site; 6) two H^+ in an octahedral site.

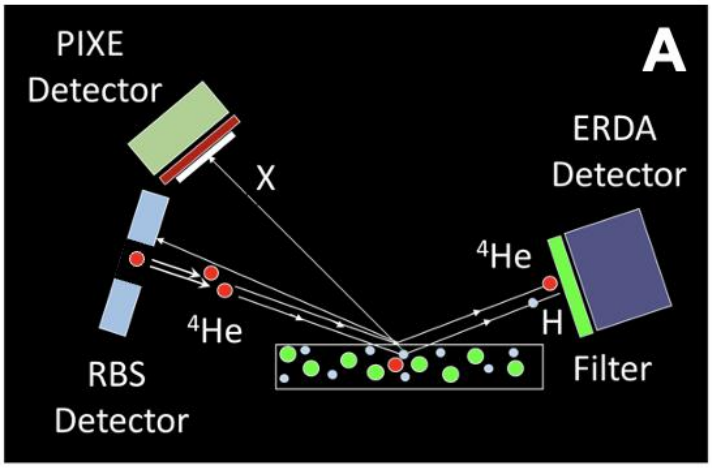
PIXE
Detector
A
X
ERDA
Detector
4He
4He
H
RBS
Detector
Filter

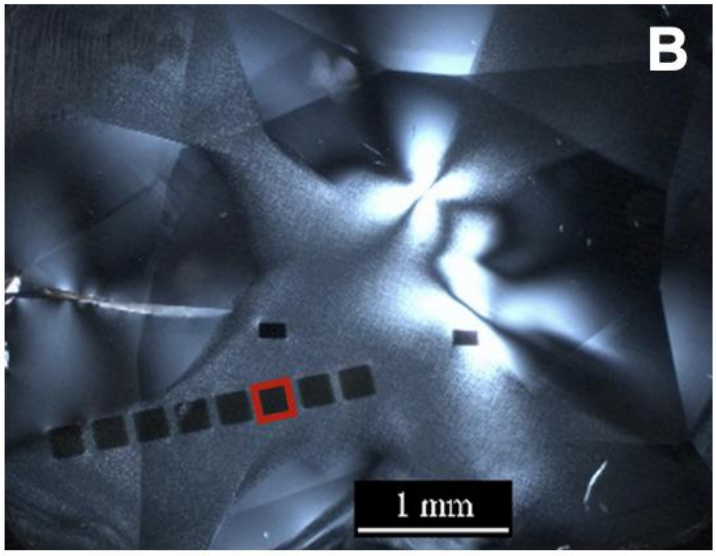
B
1 mm

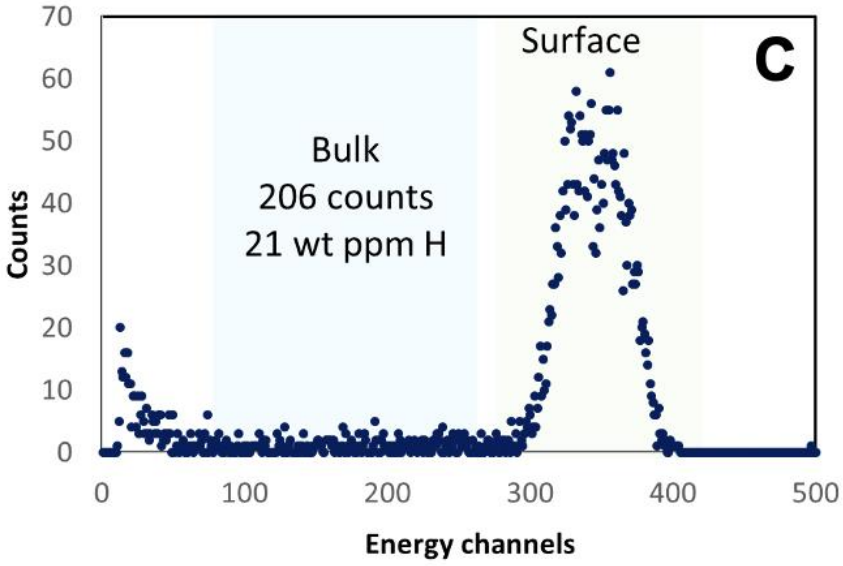
C
Surface
Bulk
206 counts
21 wt ppm H
Counts
Energy channels
0
10
20
30
40
50
60
70
0
100
200
300
400
500

402

FIGURE 2. Elastic Recoil Detection Analysis (ERDA). **(A)** Principle of ERDA. An incident 3x3μm^2 beam of $^4He^+$ at 2.8 MeV and 500 pA is scanned on the sample with a grazing angle of 30°. Three detections are simultaneously performed: particle induced X-ray emission (PIXE), Rutherford backscattering (RBS), and ERDA. More details are available in Withers et al. (2012); Bolfan-Casanova et al. (2018); and Vangu et al. (2023). **(B)** Optical picture of an asteriated diamond (Sorbonne University Collection) with two growth sectors, corresponding to octahedral (transparent areas) and cuboid (opaque gray, central star) crystal growth. The dark squares are areas analyzed by ERDA, resulting in formation of a thin graphite surface. The square outlined in red corresponds to the ERDA spectrum in (C). **(C)** Typical ERDA spectrum for a nominally anhydrous mineral, obtained in the cuboid sector of the diamond in (B). The large peak (green shaded area) results from surface contamination, while the bulk region (blue) corresponds to H contained in the sample. The 206 counts obtained in this energy range correspond to a concentration of 21 wt ppm H with a relative uncertainty of 12% (Vangu et al. 2023).

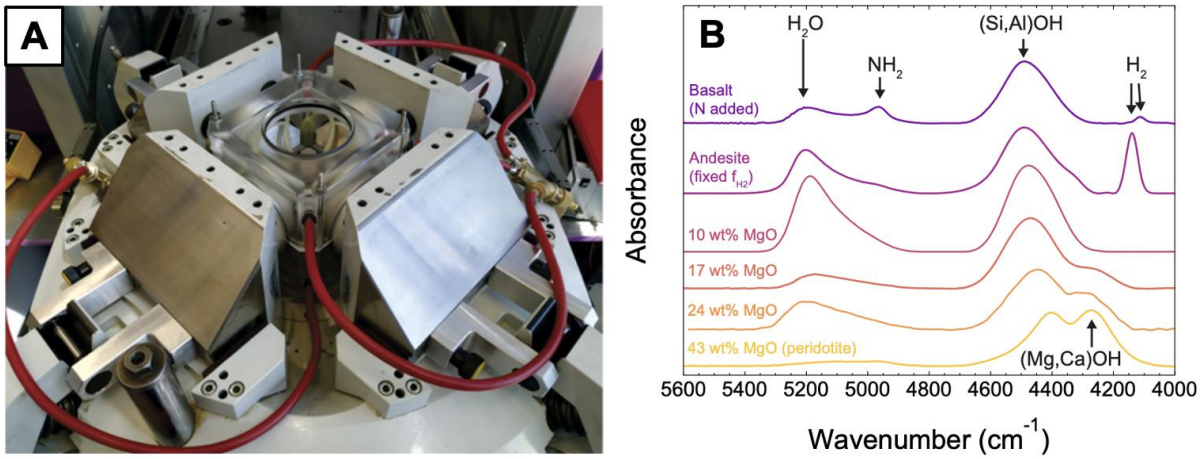

FIGURE 3 (A) Multi-anvil apparatus used to recover glasses quenched from highly depolymerized melts at high pressure (Bondar et al. 2022). Rapid quenching is achieved by modifying the anvil setup in two ways: 1) the device is cooled by circulating coolant through the volume enclosed by the plastic box that can be seen in the center of the photograph; 2) the multi-anvil cell assembly is redesigned to maximize heat transfer from the sample to the cooled exterior of the solid pressure medium. **(B)** Near infrared spectra of glasses quenched at high pressures, demonstrating different solubility mechanisms for hydrogen in melts. Top spectrum is an Fe-free basalt synthesized at 1.2 GPa at low f_{O2}, with added nitrogen; this glass contains NH_2^- groups and H_2 in addition to H_2O and OH^- groups. Second spectrum from the top is an andesitic glass recovered from 2.6 GPa, at low f_{O2} and fixed f_{H2} (Hirschmann et al. 2012). The other four glasses (Bondar et al. 2022) illustrate the effect of increasing depolymerization (with increasing MgO content) on shifting the peak position of the (Si,Al)OH band to the right, and emergence of a new band at lower frequency attributed to (Mg,Ca)OH. For comparison, spectra are arbitrarily scaled, offset, and corrected for background associated with an Fe^{2+} band at higher frequency (wavenumber) and/or the fundamental O-H stretching vibration at lower frequency.

SIDEBAR

The use of different units in the literature for specifying hydrogen concentrations can lead to confusion. Typically, geophysicists in the field of rock mechanics specify an atomic concentration using "ppm H/Si" (or H/10^6 Si, which is the same unit), while mineralogists and petrologists use "wt% H_2O" or "wt. ppm H_2O". Others yet may prefer to specify hydrogen as at. ppm H or OH, without ratioing to Si concentration (which would obviously be inapplicable to materials such as diamond or oxide minerals). Usage of a weight-based unit for minerals facilitates convenient comparison to the convention most commonly used for glasses, as well as other elemental concentrations (as listed in a table of microprobe data, for instance). However, some authors casually use the unit "ppm" without stating whether they mean atomic or wt. ppm. This problem is conveniently circumvented by using the unit "µg/g" (equivalent to wt. ppm), as preferred currently by most geochemists. For silicate phases, the articles in this issue use "wt% H_2O" or "ppm H_2O by weight" (=wt. ppm H_2O). To aid the reader in following the literature, a table for converting from one unit to another is provided below.

As an example, for a typical mantle olivine composition ($Mg_{1.8}Fe_{0.2}SiO_4$), the conversion factor from µg/g H_2O (or wt. ppm H_2O) to H/10^6 Si is 0.1119 × (147 g/mol) / (1 Si per formula unit) = 16.45.

To:	wt% H_2O	µg/g H_2O or wt ppm H_2O	H/10^6Si	at ppm H	wt ppm H
From:					
wt% H_2O	1	10^4	1119 M/N_{Si}	1119 M/N	1119
µg/g or wt ppm H_2O	10^{-4}	1	0.1119 M/N_{Si}	0.1119 M/N	0.1119
H/10^6Si	8.937×10^{-4} N_{Si}/M	8.937N_{Si}/M	1	N_{Si}/N	N_{Si}/M
at ppm H	8.937×10^{-4} N/M	8.937N/M	N/N_{Si}	1	N/M
wt ppm H	8.937×10^{-4}	8.937	M/N_{Si}	M/N	1
M = molecular mass of one mineral formula unit; N_{Si} = Si per formula unit, N = atoms per formula unit					